Supporting Information

Gannoun et al. 10.1073/pnas.1017332108

SI Materials and Methods

Sample Selection and Dissolution. Enstatite chondrites consist of highly reduced mineral assemblages formed under very low oxygen fugacity (fO_2) conditions. They are classified into two subgroups on the basis of the Fe/Si bulk ratios: the high-Fe, high siderophile group (EH) and low Fe, low siderophile group (EL). Both EH and EL comprise a series of members from unequilibrated to highly equilibrated ones. The EL chondrites contain more highly equilibrated members than the EH chondrites. Thirteen enstatites chondrites belonging to both EH and EL subgroups were investigated during this study. This suite comprises eight unequilibrated samples (EH3, EL3) and five of other petrographic type (from type 4 to 6). Additionally, one ordinary chondrite (Jilin, H5) and one carbonaceous chondrite (Allende, CV3) were also analyzed during this study for the sake of comparison. Chondrite samples analyzed for Sm–Nd systematics and measured $^{147}Sm/^{144}Nd$ ratios are presented in Table S1. Different digestion techniques have been tested in the past to dissolve the carbonaceous chondrite Allende: (*i*) sealed beaker on hot plate using a mixture of $HF{:}HNO_3$ concentrated acid, (*ii*) again the same reagents but in bombs (higher pressure-temperature conditions), and (*iii*) fusion. Although this sample contains a large amount of both refractory inclusions and presolar grains, no difference has been found. In fact we measured each time very slightly different Sm and Nd isotope composition but this can be explained by the heterogeneity of the powder itself. The isotope heterogeneity at the bulk sample size (dissolution around 100 mg to 1 g) is also illustrated in Fig. S1. The large range of $^{143}Nd/^{144}Nd$ and $^{147}Sm/^{144}Nd$ ratios measured for different dissolution of Allende indicates that this sample is not homogeneous, even when a large quantity of powder is used for dissolution (about 1 g). But this range is not due to incomplete dissolution of refractory phases. Because of its low blank and reliable isotope data results we opt for steel-jacketed tetrafluoroethylene (TFE) Teflon lined Parr bombs for sample digestion.

About one gram of homogenized powdered samples were dissolved in a $HF–HNO_3$ mixture in the proportions of 9:3 in steel-jacketed TFE Teflon lined Parr bombs. Samples were digested in an oven at 150 °C for not less than 72 h. The solution is dried after the add of few mL of $HClO_4$ and the residue redissolved with the mixture of HCl and HNO_3 ultrapure acids in the proportions 1:2, transferred in Savillex perfluoroalkoxy 60 mL beakers. The beakers were placed in an oven at 150 °C for 48 h. Once a clear solution was obtained, a 5% aliquot was taken and spiked with $^{149}Sm–^{150}Nd$ tracer to measure Sm and Nd concentrations by isotope dilution. This spike was calibrated against standard solutions prepared from AMES and JNdi-1. Sm and Nd results on Allende using this spike are concordant with literature values (Fig. S1).

Chemical Separation and Purification of Sm and Nd. The full chemical procedure for the extraction and purification of Sm and Nd followed closely techniques described previously (1). The Sm and Nd fractions were separated with a two stage-chemistry procedure. In the first stage rare earth elements (REEs) as a group were separated by using cation resin and HCl. The REE split were then processed two times through a cation column using 2-Methylactic acid (0.2M and pH = 4.7) with a small amount of H_2O_2 to ensure perfect separation of Nd from Ce and Sm by reducing the effect of interferences on mass 142 (from Ce) and on mass 144, 148 and 150 from Sm. The last step consists on one pass trough Ln-spec resin in week HCl acid. Organic residues are then completely removed and the sample is ready to be loaded on Re filament. Unspiked Sm fraction from each chondrite sample was also purified using the same technique. Total procedural blanks for Sm and Nd were 1.5 and 8.3 pg, respectively. The percentage blank contribution to each sample was always less than 0.02‰, so no blank correction has been applied. The spiked fractions have been separated using the method developed by Pin et al. (2). Ce and Sm interferences on masses 142 and 144 and expressed in ppm are indicated in Table S1. Sm interferences are negligible whereas for a few samples the Ce signal accounts for more than a few tens ppm on mass 142. The Ce signal decreases rapidly during the isotope measurement. Fig. S2 shows that there is no covariation between $^{142}Nd/^{144}Nd$ ratios and either $^{142}Ce/^{142}Nd$ or $^{144}Sm/^{144}Nd$ ratios.

As for Nd, the purified fractions of Sm obtained using 2-Methylactic acid were passed through Ln-spec resin and eluted in 0.5N HCl to discard all organic residues.

Mass Spectrometry. All the isotopic measurements presented in this study were obtained on the Thermo-Fisher Triton thermal ionization mass spectrometer at Laboratoire Magmas et Volcans. The purified Sm and Nd cuts were loaded in 2.5N HCl on outgassed zone-refined Re filaments. The Nd was measured in static mode by using the nine faraday cups, as positive metal ions following the configuration presented below. Nd isotope measurements using both dynamic and static modes have been compared. No significant difference has been observed for the measurement of 3.8 Ga old samples coming from the Isua supracrustal belt (SW Greenland) that present ^{142}Nd excesses of about 15 ppm (3). Because enstatite chondrites present the lowest Nd contents among chondrites, we have decided to use a static procedure for a better ion-counting statistic. The Farady cup configuration used for Nd isotope measurements (mass) as follows: L4, ^{140}Ce; L3, ^{142}Nd; L2, ^{143}Nd; L1, ^{144}Nd; C, ^{145}Nd; H1, ^{146}Nd; H2, ^{147}Sm; H3, ^{148}Nd; H4, ^{150}Nd.

To test the robustness of the Nd isotope data obtained by static mode, we have analyzed several fractions of JNdi-1 standard enriched artificially with known amount of ^{142}Nd spike. The results are plotted in Fig. S3 and show that even for low amount of Nd (100 ng), artificial excesses of ^{142}Nd as low as 17 ppm can be resolved.

All measured data were corrected for instrumental mass fractionation using the exponential law and $^{146}Nd/^{144}Nd = 0.7219$ (Table S1). Each measurement consists of 27 blocks of 20 ratios (approximately 8 s for integration time) using the amplifier rotation and taking the background before each block. Gain was taken before the beginning of each run. The ^{142}Nd signals range between 0.9 and 4.5×10^{-11} A for all chondrite samples. The $^{142}Nd/^{144}Nd$ data are expressed in ppm relative to the mean value obtained on the JNdi-1 standards measured during the same campaign. Our current mean value for $^{142}Nd/^{144}Nd$ in the JNdi-1 standard is 1.1418331 ± 0.0000066 ($2\sigma_m$). The external reproducibility on repeated standard analyses is always better than 6 ppm for the given campaign. No orrelation is observed between the different Nd ratios (Fig. S4).

The Sm was measured in static mode as Sm^+ ions using double Re filaments following the cup configuration presented here: L4, ^{144}Sm; L3, ^{146}Nd; L2, ^{147}Sm; L1, ^{148}Sm; C, ^{149}Sm; H1, ^{150}Sm; H2, ^{152}Sm; H3, ^{154}Sm; H4, ^{156}Gd.

Each run consists of 9 blocks of 20 cycles using the amplifier rotation and taking the background before each block. The ^{152}Sm signals range between 0.3 and 1.9×10^{-11} A. Possible isobaric interferences from Nd and Gd were monitored by measuring the intensity on ^{146}Nd and ^{156}Gd masses (Table S2). Sm data were corrected for instrumental mass fractionation using the exponential law and $^{147}Sm/^{152}Sm = 0.56081$. Sm isotope compositions for both standards and samples are given in Table S2. Sm isotope compositions have been measured during two different periods. Internal errors are higher in the first sequence of measurement than in the second one. We have encountered a problem with the faraday cups during the first sequence of measurements. Then these samples have been measured twice and the Sm isotope composition presented in Table S2 for sequence 1 corresponds to the second run. Because most of samples have been measured at very low intensity ($^{152}Sm < 0.4$ V), $^{144}Sm/^{152}Sm$ ratios have large errors. This is the reason why these samples have not been represented in the diagram presented in Fig. S5.

We have also calculated the Sm isotope ratios relative to ^{154}Sm (100% r-process) and all data are fractionation corrected using the exponential law and $^{147}Sm/^{154}Sm = 0.65918$. Using this normalization scheme (Table S2), the deviations expressed in μ-notation (ppm deviation relative to the ratio measured in terrestrial standard) are similar to those from previous calculation within the error bar.

Correction on $^{142}Nd/^{144}Nd$ Ratios. Exposure to galactic cosmic rays modifies a sample's Sm and Nd isotopic composition and its $^{142}Nd/^{144}Nd$ ratio. A long exposure age tends to decrease the $^{142}Nd/^{144}Nd$ ratio as observed in lunar samples (4). The secondary neutron capture effect is currently quantified using Sm isotope measurements because ^{149}Sm has the largest thermal neutron capture cross section (e.g., ref. 5). The neutron capture effect is clearly seen in a negative correlation between $^{150}Sm/^{152}Sm$ and $^{149}Sm/^{152}Sm$ ratios (Fig. S5), but ^{149}Sm deficits are lower than −1.5 epilson-unit, which corresponds to a correction smaller than 1 ppm on the $^{142}Nd/^{144}Nd$ ratios following the method developed by Nyquist et al. (6) or Rankenburg et al. (7). As is clearly demonstrated in the ^{149}Sm–^{150}Sm isotope diagram, several samples do not plot on the correlation line and the observed scatter could reflect isotope heterogeneities in the solar nebula when chondrites were formed.

The $^{142}Nd/^{144}Nd$ ratios presented in Fig. 1*B* have been corrected for a common evolution considering a constant $^{147}Sm/^{144}Nd$ ratio [0.196 (8) from 4.568 Ga and an initial solar system $^{146}Sm/^{144}Sm$ ratio equal to 0.0085 (9). The $^{147}Sm/^{144}Nd$ ratio considered for each sample is not the ratio measured on the aliquot but this ratio has been recalculated using measured $^{143}Nd/^{144}Nd$ ratio and assuming that these samples have evolved from the same chondritic reservoir (present day values are 0.1960 and 0.512630 for $^{147}Sm/^{144}Nd$ ratio and $^{143}Nd/^{144}Nd$ ratios, respectively (8)]. Measured $^{142}Nd/^{144}Nd$ ratios are compared to corrected $^{142}Nd/^{144}Nd$ ratios in Table S3. The $^{142}Nd/^{144}Nd$ ratios reported in Fig. 1*A* are those from the first column whereas in all other diagrams we have plotted corrected $^{142}Nd/^{144}Nd$ ratios presented in the last column of the Table S3.

1. Boyet M, Carlson RW (2005) ^{142}Nd evidence for early (>4.53 Ga) global differentiation of the silicate earth. *Science* 309:576–581.
2. Pin C, Santos Zalduegui JF (1997) Sequential separation of light rare-earth elements, thorium and uranium by miniaturized extraction chromatography: Application to isotopic analyses of cilicate rocks. *Anal Chim Acta* 339:79–89.
3. Rizo Garza HL, Boyet MM, Blichert-Toft J, Rosing M, Gannoun A (2010) A coupled Nd and Hf isotopic study of Isua Archean rocks and the differentiation of the Hadean mantle. AGU Fall Meeting (American Geophysical Union, San Francisco).
4. Boyet M, Carlson RW (2007) Early lunar differentiation and a non magma ocean origin for the lunar crust. *Earth Planet Sci Lett* 262:505–516.
5. Lingenfelter RE, Canfield EH, Hampel VE (1972) The lunar neutron flux revisited. *Earth Planet Sci Lett* 16:335–369.
6. Nyquist LE, et al. (1995) ^{146}Sm-^{142}Nd formation interval for the lunar mantle material. *Geochim Cosmochim Acta* 59:2817–2837.
7. Rankenburg K, Brandon AD, Neal CR (2006) Neodymium isotope evidence for a chondritic composition of the moon. *Science* 312:1369–1372.
8. Bouvier A, Vervoort JD, Patchett PJ (2008) The Lu–Hf and Sm–Nd isotopic composition of CHUR: Constraints from unequilibrated chondrites and implications for the bulk composition of terrestrial planets. *Earth Planet Sci Lett* 273:48–57.
9. Boyet M, Carlson RW, Horan M (2010) Old Sm–Nd ages for cumulate eucrites and redetermination of the solars system initial $^{146}Sm/^{144}Sm$ ratio. *Earth Planet Sci Lett* 291:172–181.

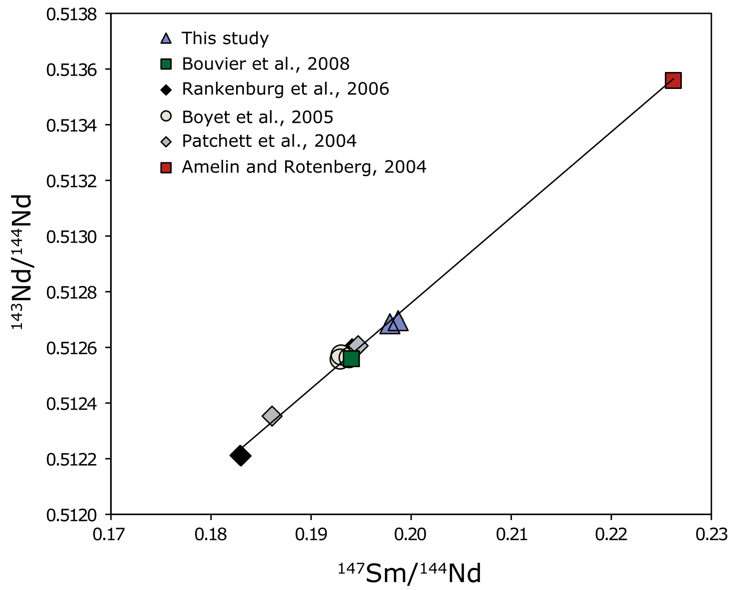

Fig. S1. The $^{147}Sm/^{144}Nd$–$^{143}Nd/^{144}Nd$ ratios obtained on Allende (CV3). Comparison of different dissolutions made by different laboratories. Source of literature data (1–5).

1 Boyet M, Carlson RW (2005) ^{142}Nd evidence for early (>4.53 Ga) global differentiation of the silicate earth. *Science* 309:576–581.
2 Rankenburg K, Brandon AD, Neal CR (2006) Neodymium isotope evidence for a chondritic composition of the moon. *Science* 312:1369–1372.
3 Patchett PJ, Vervoort JD, Soderlund U, Salters VJM (2004) Lu–Hf and Sm–Nd isotopic systematics in chondrites and their constraints on the Lu–Hf properties of the Earth. *Earth Planet Sc Lett* 222:29–41.
4 Amelin Y, Rotenberg E (2004) Sm–Nd systematics of chondrites. *Earth Planet Sc Lett* 223:267–282.
5 Bouvier A, Vervoort JD, Patchett PJ (2008) The Lu–Hf and Sm–Nd isotopic composition of CHUR: Constraints from unequilbrated chondrites and implications for the bulk composition of terrestrial planets. *Earth Planet Sci Lett* 273:48–57.

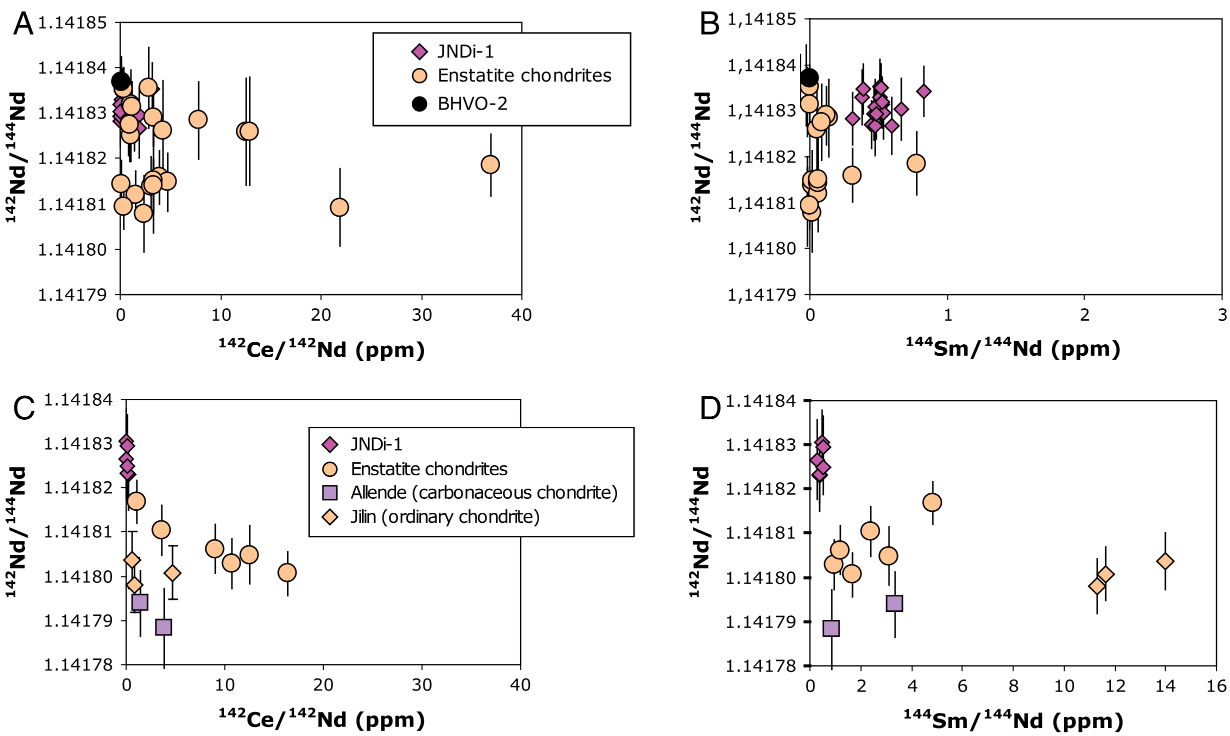

Fig. S2. The $^{142}Nd/^{144}Nd$ ratios corrected from isobaric interferences vs the Ce and Sm contribution for standards and samples measured in sequence 1 (*A* and *B*) and 2 (*C* and *D*). Interferences are expressed in ppm. The highest ^{142}Ce interference has been measured in Eagle and this sample has been measured only once. However the two measurements of St. Mark's have been realized during the first sequence of analyses. Although the Ce interference accounts for 20 ppm in the first measurement and is negligible in the second run, we have measured the same $^{142}Nd/^{144}Nd$ ratios. We conclude that Ce and Sm interferences, when they are present, are perfectly corrected.

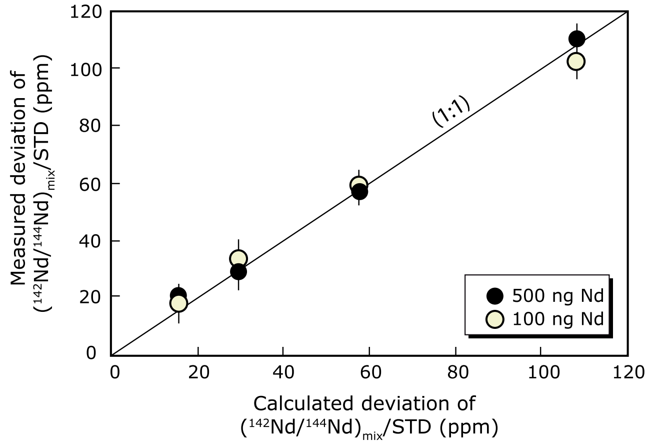

Fig. S3. Calculated $^{142}Nd/^{144}Nd$ deviation of artificially enriched JNdi-1 standard (100 nd 500 ng of total Nd) versus the measured deviation.

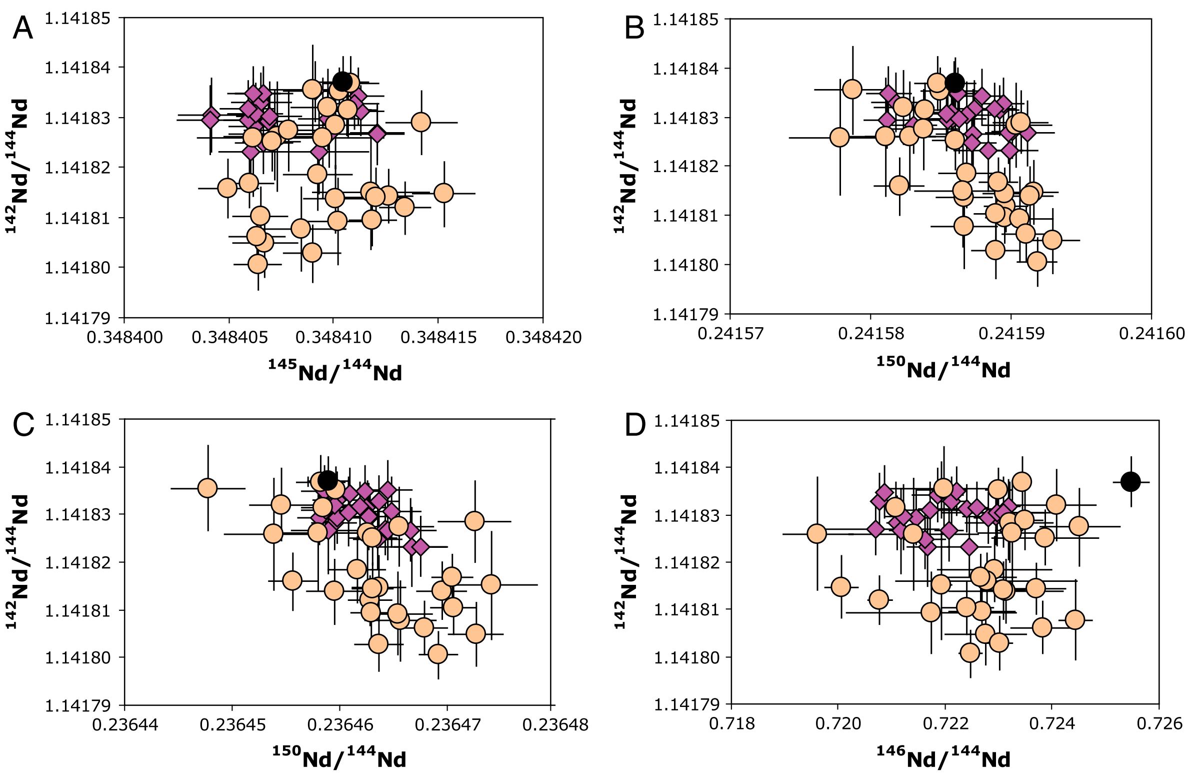

Fig. S4. Nd isotope ratios measured for the JNdi-1 standard, BHVO-2 (terrestrial basalt) and meteorite samples. The $^{142}Nd/^{144}Nd$, $^{145}Nd/^{144}Nd$, $^{148}Nd/^{144}Nd$, $^{150}Nd/^{144}Nd$ ratios are corrected for instrumental mass fractionation (*A*, *B*, and *C*). In *D*, the raw $^{146}Nd/^{144}Nd$ ratios are plotted. Symbols as in Fig. S2.

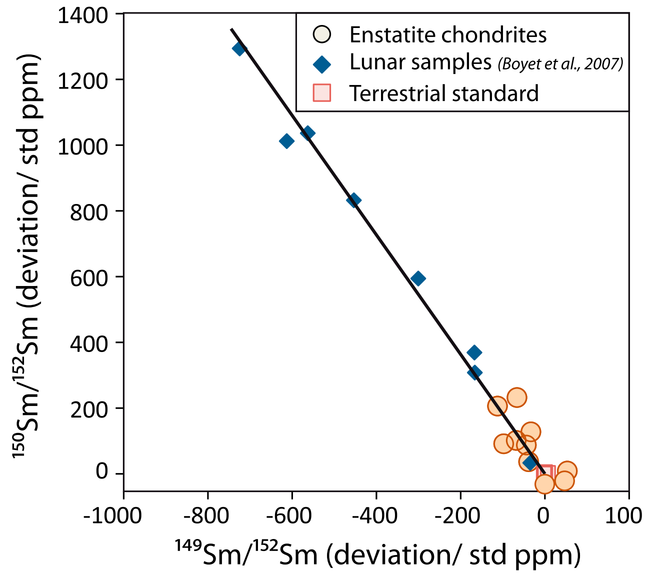

Fig. S5. The $^{149}Sm/^{152}Sm$ vs. $^{150}Sm/^{152}Sm$ isotopic covariation for lunar samples and enstatite chondrites.

Table S1. The $^{147}Sm/^{144}Nd$ ratios and concentration data for enstatite chondrites analyzed in this study

Sample	Type	Source	Weight (g)	Sm (ppm)	Nd (ppm)	$^{147}Sm/^{144}Nd$
ALHA 77295	EH3	NASA	0.9135	0.1411	0.4330	0.1970
ALHA duplicate			0.9150	0.1143	0.3439	0.2009
Allende	CV3	Smith. Inst. *	1.0018	0.2406	0.7350	0.1979
Eagle 4739	EL6 Fall	AMNH †	0.9147	0.1078	0.3256	0.2001
Hvittis	EL6	dealers	0.9136	0.1199	0.3611	0.2007
Indarch	EH4	NHM ‡	0.9577	0.1013	0.3050	0.2009
Jilin	H5 Fall	NHM	1.1489	0.1732	0.5500	0.1904
Khairpur	EL6 Fall	NHM	0.9696	0.1336	0.4111	0.1965
Kota-Kota	EH3	NHM	0.9290	0.1951	0.7040	0.1675
Kota-Kota duplicate			0.9011	0.2018	0.7309	0.1669
MAC 02837	EL3	NASA	0.9370	0.1634	0.4972	0.1987
MAC 02839	EL3	NASA	1.0544	0.1871	0.5723	0.1976
MAC 88180	EL3	NASA	0.9273	0.2673	0.8187	0.1974
Sahara 97072	EH3	dealers	0.9158	0.1533	0.4942	0.1875
Sahara 97096	EH3	dealers	1.1729	0.1396	0.4305	0.1961
Sahara 97158	EH3	dealers	0.9408	0.1383	0.4404	0.1899
St. Mark's 4804	EH5 Fall	AMNH	0.9572	0.1460	0.4519	0.1953

*Smithsonian Institution.
†American Museum of Natural History.
‡Natural History Museum of London.

Table S2. Measured Nd isotope composition of standards and samples

	Int. ^{142}Nd (V)	^{142}Ce/^{142}Nd (ppm)	^{144}Sm/^{144}Nd (ppm)	^{142}Nd/^{144}Nd	2s	μ^{142}Nd (ppm)	2s (ppm)	^{143}Nd/^{144}Nd	2s	^{145}Nd/^{144}Nd	2s	μ^{145}Nd (ppm)	2s (ppm)	^{148}Nd/^{144}Nd	2s	μ^{148}Nd (ppm)	2s (ppm)	^{150}Nd/^{144}Nd	2s	μ^{150}Nd (ppm)	2s (ppm)	^{146}Nd/^{144}Nd	2s
Sequence 1																							
JNDi-1 std.	3.8	1.5	0.4	1.141827	0.000005	−3.5	4.6	0.512103	0.000002	0.348412	0.000001	10.0	3.7	0.241590	0.000001	14.7	6.0	0.236464	0.000002	10.9	8.2	0.72071	0.00117
JNDi-1 std.	4.6	0.8	0.5	1.141831	0.000005	0.3	4.4	0.512105	0.000002	0.348411	0.000001	7.7	3.2	0.241589	0.000001	11.0	5.6	0.236462	0.000002	3.8	7.4	0.72240	0.00090
JNDi-1 std.	4.0	0.2	0.8	1.141834	0.000006	2.8	4.8	0.512104	0.000002	0.348411	0.000001	7.5	3.5	0.241588	0.000001	5.9	6.0	0.236461	0.000002	−2.8	8.2	0.72185	0.00047
JNDi-1 std.	3.0	0.2	0.4	1.141833	0.000006	1.7	5.2	0.512104	0.000002	0.348407	0.000001	−5.8	4.0	0.241582	0.000002	−19.6	7.1	0.236460	0.000002	−8.0	9.3	0.72078	0.00013
JNDi-1 std.	3.5	0.1	0.4	1.141835	0.000005	3.3	4.8	0.512104	0.000002	0.348407	0.000001	−5.5	3.9	0.241581	0.000002	−21.7	6.6	0.236459	0.000002	−12.6	9.1	0.72086	0.00008
JNDi-1 std.	3.8	0.0	0.3	1.141828	0.000006	−2.4	4.9	0.512101	0.000002	0.348406	0.000001	−6.8	3.4	0.241583	0.000002	−14.1	6.5	0.236459	0.000002	−8.9	8.5	0.72110	0.00018
JNDi-1 std.	3.6	0.0	0.5	1.141829	0.000006	−1.4	4.9	0.512102	0.000002	0.348406	0.000001	−7.6	3.4	0.241581	0.000002	−22.2	6.6	0.236458	0.000002	−14.7	8.5	0.72145	0.00022
JNDi-1 std.	4.5	0.1	0.5	1.141833	0.000005	1.6	4.4	0.512106	0.000002	0.348411	0.000001	6.9	3.4	0.241589	0.000001	12.3	5.7	0.236464	0.000002	8.6	7.9	0.72212	0.00030
JNDi-1 std.	4.1	0.1	0.5	1.141832	0.000005	0.6	4.5	0.512107	0.000002	0.348411	0.000001	5.9	3.3	0.241589	0.000002	9.4	6.3	0.236462	0.000002	1.0	8.4	0.72260	0.00018
JNDi-1 std.	2.9	3.2	0.5	1.141835	0.000006	3.7	5.2	0.512103	0.000002	0.348409	0.000002	1.6	4.3	0.241586	0.000002	−2.4	7.0	0.236464	0.000002	12.1	9.4	0.72192	0.00046
JNDi-1 std.	3.1	1.9	0.5	1.141830	0.000006	−1.2	5.2	0.512101	0.000002	0.348410	0.000001	3.3	4.0	0.241586	0.000002	−2.7	7.1	0.236463	0.000002	5.2	9.1	0.72294	0.00060
JNDi-1 std.	2.7	1.9	0.5	1.141827	0.000007	−3.8	5.7	0.512103	0.000002	0.348410	0.000001	3.5	4.3	0.241591	0.000002	19.4	7.7	0.236467	0.000002	21.2	9.9	0.72207	0.00026
JNDi-1 std.	3.4	0.8	0.6	1.141827	0.000006	−3.7	5.3	0.512106	0.000002	0.348412	0.000001	10.0	3.8	0.241590	0.000002	13.6	6.7	0.236464	0.000002	12.0	8.8	0.72319	0.00024
JNDi-1 std.	3.5	1.0	0.5	1.141831	0.000006	−0.1	5.2	0.512104	0.000002	0.348406	0.000001	−6.6	3.8	0.241586	0.000002	−3.2	6.7	0.236459	0.000002	−12.0	9.6	0.72172	0.00060
JNDi-1 std.	4.0	0.4	0.5	1.141835	0.000005	3.4	4.5	0.512104	0.000002	0.348406	0.000001	−6.9	3.5	0.241586	0.000001	−1.4	6.0	0.236462	0.000002	3.4	8.1	0.72220	0.00015
JNDi-1 std.	3.7	0.0	0.5	1.141829	0.000005	−1.5	4.7	0.512105	0.000002	0.348407	0.000001	−4.9	3.5	0.241586	0.000002	−4.1	6.4	0.236460	0.000002	−7.6	8.6	0.72280	0.00025
JNDi-1 std.	3.9	0.0	0.5	1.141832	0.000006	0.7	4.9	0.512105	0.000002	0.348406	0.000001	−7.7	3.7	0.241587	0.000001	3.7	6.1	0.236460	0.000002	−8.7	8.7	0.72317	0.00022
JNDi-1 std.	3.8	−0.1	0.7	1.141830	0.000007	−0.6	5.9	0.512105	0.000002	0.348407	0.000002	−4.7	4.4	0.241587	0.000002	1.5	7.1	0.236461	0.000002	−3.0	9.8	0.72296	0.00101
Average (n = 18)				1.141831	0.000006	0.0	4.9	0.512104	0.000003	0.348409	0.000005	0.0	13.6	0.241587	0.000006	0.0	25.6	0.236462	0.000005	0.0	20.6	0.72205	0.00164
Allende run#1	3.1	0.3	0.0	1.141807	0.000006	−21.2	5.3	0.512667	0.000002	0.348405	0.000001	−10.4	3.9	0.241588	0.000002	5.7	7.0	0.236461	0.000002	−1.2	9.5	0.72372	0.00041
Allende run#2	2.6	0.5	0.1	1.141805	0.000007	−22.6	5.9	0.512666	0.000002	0.348409	0.000002	0.6	4.5	0.241589	0.000002	11.7	7.3	0.236464	0.000002	12.2	10.2	0.72354	0.00031
Allende run#3	2.8	0.5	−0.1	1.141806	0.000009	−21.5	7.9	0.512670	0.000003	0.348410	0.000002	4.5	5.5	0.241593	0.000002	25.2	9.7	0.236469	0.000004	31.2	15.1	0.72344	0.00025
Average				1.141806	0.000002	−21.8	1.5	0.512668	0.000004	0.348408	0.000005	−1.8	15.4	0.241590	0.000005	14.2	19.9	0.236465	0.000008	14.1	32.5	0.72357	0.00028
ALHA77295	2.2	7.8	0.1	1.141828	0.000008	−2.3	7.4	0.512607	0.000003	0.348410	0.000002	4.3	5.8	0.241590	0.000003	16.1	10.4	0.236473	0.000003	46.4	14.1	0.72320	0.00082
Eagle 4729	1.2	37.0	0.8	1.141819	0.000007	−10.9	6.0	0.512696	0.000003	0.348409	0.000002	1.9	4.7	0.241587	0.000002	1.5	8.3	0.236462	0.000003	0.1	11.2	0.72292	0.00106
Indarch run#1	2.5	3.0	0.0	1.141814	0.000007	−15.1	5.9	0.512626	0.000007	0.348410	0.000002	4.3	4.3	0.241587	0.000002	0.7	8.2	0.236460	0.000003	−8.7	10.8	0.72313	0.00107
Indarch run#2	1.8	2.4	0.0	1.141808	0.000008	−20.4	7.3	0.512621	0.000008	0.348408	0.000002	−0.3	6.0	0.241587	0.000002	0.7	9.7	0.236466	0.000003	17.2	13.9	0.72444	0.00030
Average				1.141811	0.000008	−17.7	7.4	0.512624	0.000006	0.348409	0.000002	2.0	6.4	0.241587	0.000002	0.7	0.1	0.236463	0.000009	4.3	36.6	0.72379	0.00185
Hvittis	2.9	3.4	0.1	1.141829	0.000006	−1.8	5.5	0.512750	0.000003	0.348414	0.000002	16.1	4.9	0.241591	0.000002	17.3	8.1	0.236490	0.000002	119.8	10.2	0.72350	0.00032
Khairpur	1.6	3.9	0.3	1.141816	0.000006	−13.2	5.1	0.512633	0.000002	0.348405	0.000001	−10.3	4.1	0.241582	0.000002	−18.5	7.2	0.236456	0.000002	−25.4	9.5	0.72277	0.00170
Kota-Kota run#1	1.5	2.9	0.0	1.141836	0.000009	4.0	7.8	0.512456	0.000003	0.348409	0.000002	1.2	5.8	0.241579	0.000003	−32.3	11.0	0.236448	0.000003	−58.5	14.6	0.72198	0.00119
Kota-Kota run#2	1.9	1.1	0.0	1.141832	0.000008	0.9	6.6	0.512458	0.000003	0.348410	0.000002	3.3	5.0	0.241582	0.000002	−17.1	8.9	0.236455	0.000003	−29.5	12.8	0.72408	0.00073
Average				1.141834	0.000005	2.4	4.4	0.512457	0.000002	0.348409	0.000001	2.2	2.9	0.241581	0.000005	−24.7	21.5	0.236451	0.000010	−44.0	40.9	0.72303	0.00297
Mac 02837 run#1	1.0	12.6	0.1	1.141826	0.000012	−4.5	10.2	0.512653	0.000004	0.348406	0.000003	−7.0	7.5	0.241578	0.000004	−36.0	14.7	0.236454	0.000005	−32.4	19.8	0.72140	0.00121
Mac 02837 run#2	1.1	4.3	−0.3	1.141826	0.000011	−4.3	9.6	0.512653	0.000004	0.348407	0.000003	−3.6	7.3	0.241583	0.000003	−15.6	12.9	0.236463	0.000004	4.2	16.7	0.72326	0.00064
Average				1.141826	0.000000	−4.4	0.3	0.512653	0.000000	0.348407	0.000002	−5.3	4.8	0.241580	0.000007	−25.8	29.0	0.236458	0.000012	−14.1	51.8	0.72233	0.00263

	Int. ^{142}Nd (V)	$^{142}Ce/^{142}Nd$ (ppm)	$^{144}Sm/^{144}Nd$ (ppm)	$^{142}Nd/^{144}Nd$	2s	$\mu^{142}Nd$ (ppm)	2s (ppm)	$^{143}Nd/^{144}Nd$	2s	$^{145}Nd/^{144}Nd$	2s	$\mu^{145}Nd$ (ppm)	2s (ppm)	$^{148}Nd/^{144}Nd$	2s	$\mu^{148}Nd$ (ppm)	2s (ppm)	$^{150}Nd/^{144}Nd$	2s	$\mu^{150}Nd$ (ppm)	2s (ppm)	$^{146}Nd/^{144}Nd$	2s
Mac 02839 run#1	0.9	12.9	−0.1	1.141826	0.000012	−4.4	10.5	0.512640	0.000005	0.348409	0.000003	2.6	8.3	0.241581	0.000004	−22.4	14.5	0.236458	0.000005	−15.1	19.5	0.71962	0.00065
Mac 02839 run#2	3.4	1.1	−0.2	1.141825	0.000006	−5.1	5.0	0.512642	0.000002	0.348407	0.000001	−4.4	3.9	0.241586	0.000002	−1.9	6.6	0.236463	0.000002	6.4	9.1	0.72387	0.00100
Mac 02839 run#3	1.9	0.9	0.1	1.141827	0.000008	−3.1	7.2	0.512644	0.000003	0.348408	0.000002	−2.1	6.1	0.241584	0.000003	−11.3	10.6	0.236466	0.000003	16.7	13.5	0.72452	0.00075
Average				1.141826	0.000002	−4.2	2.1	0.512642	0.000003	0.348408	0.000002	−1.3	7.1	0.241584	0.000005	−11.9	20.5	0.236462	0.000008	2.7	32.4	0.72267	0.00532
Mac 88180 run#1	3.7	1.2	0.0	1.141831	0.000005	0.4	4.8	0.512730	0.000002	0.348411	0.000001	6.1	3.7	0.241584	0.000002	−11.0	6.3	0.236458	0.000002	−13.2	8.6	0.72108	0.00008
Mac 88180 run#2	4.0	0.3	0.0	1.141835	0.000005	3.7	4.1	0.512732	0.000002	0.348410	0.000001	4.9	3.0	0.241585	0.000001	−6.6	5.4	0.236460	0.000002	−8.3	7.3	0.72299	0.00024
Mac 88180 run#3	3.2	0.2	−0.1	1.141837	0.000005	5.1	4.8	0.512733	0.000002	0.348411	0.000001	6.4	3.7	0.241585	0.000002	−7.1	7.1	0.236458	0.000002	−14.1	9.3	0.72345	0.00011
Average				1.141834	0.000005	3.1	4.8	0.512732	0.000003	0.348411	0.000001	5.8	1.6	0.241585	0.000001	−8.2	4.8	0.236459	0.000001	−11.9	6.3	0.72251	0.00251
Sahara 97072 run#1	2.9	4.8	0.0	1.141815	0.000006	−14.2	5.7	0.512518	0.000002	0.348415	0.000001	19.2	4.3	0.241592	0.000002	21.1	7.2	0.236464	0.000002	8.7	10.3	0.72006	0.00030
Sahara 97072 run#2	4.3	1.5	0.1	1.141812	0.000005	−16.7	4.5	0.512517	0.000002	0.348413	0.000001	13.8	3.4	0.241590	0.000002	13.0	6.4	0.236463	0.000002	5.1	8.5	0.72078	0.00023
Sahara 97072 run#3	4.2	0.3	0.0	1.141809	0.000005	−18.9	4.5	0.512518	0.000002	0.348412	0.000001	9.4	3.2	0.241590	0.000001	12.5	5.7	0.236463	0.000002	5.8	7.9	0.72268	0.00061
Sahara 97072 run#4	4.1	0.1	0.1	1.141814	0.000005	−14.5	4.7	0.512519	0.000002	0.348413	0.000001	11.7	3.3	0.241590	0.000001	12.4	6.2	0.236463	0.000002	6.1	8.0	0.72371	0.00054
Average				1.141813	0.000005	−16.1	4.3	0.512518	0.000002	0.348413	0.000003	13.5	8.4	0.241590	0.000002	14.7	8.4	0.236463	0.000001	6.4	3.1	0.72181	0.00336
Sahara 97158	0.9	3.3	0.1	1.141815	0.000011	−13.9	9.9	0.512561	0.000004	0.348412	0.000003	9.2	8.0	0.241587	0.000003	0.3	14.1	0.236474	0.000004	53.1	17.9	0.72193	0.00018
St. Mark's run#1	1.6	21.9	0.0	1.141809	0.000009	−19.1	7.5	0.512604	0.000003	0.348410	0.000002	4.7	5.8	0.241591	0.000002	17.2	9.7	0.236465	0.000003	16.1	13.6	0.72174	0.00159
St. Mark's run#2	3.0	3.3	0.0	1.141814	0.000006	−14.9	5.2	0.512605	0.000002	0.348412	0.000001	9.9	4.2	0.241591	0.000002	19.9	6.8	0.236469	0.000002	33.4	9.6	0.72309	0.00039
Average				1.141812	0.000007	−17.0	5.9	0.512604	0.000002	0.348411	0.000003	7.3	7.3	0.241591	0.000001	18.6	3.8	0.236467	0.000006	24.8	24.4	0.72242	0.00191
BHVO2	3.9	0.1	0.0	1.141837	0.000005	5.2	4.5	0.512983	0.000002	0.348410	0.000001	5.4	3.5	0.241586	0.000001	−2.0	5.9	0.236459	0.000002	−11.2	8.1	0.725470	0.00033
Sequence 2																							
JNDi-1 std.	2.8	0.7	0.7	1.141823	0.000008	−2.8	7.2	0.512095	0.000003	0.348409	0.000002	8.8	6.6	0.241588	0.000002	3.9	10.1	0.236467	0.000003	11.2	13.3	0.72168	0.00039
JNDi-1 std.	2.6	0.3	0.4	1.141823	0.000006	−2.7	5.5	0.512096	0.000003	0.348406	0.000001	−0.6	4.2	0.241590	0.000002	10.3	8.2	0.236468	0.000003	14.8	10.6	0.72245	0.00041
JNDi-1 std.	2.0	0.3	1.7	1.141827	0.000009	0.3	7.8	0.512098	0.000003	0.348407	0.000002	2.7	6.3	0.241587	0.000003	−0.6	10.7	0.236459	0.000003	−21.6	14.2	0.72116	0.00019
JNDi-1 std.	2.3	0.2	0.8	1.141831	0.000007	3.7	6.4	0.512102	0.000003	0.348404	0.000002	−6.0	4.5	0.241585	0.000002	−8.2	8.5	0.236465	0.000003	3.5	11.2	0.72308	0.00076
JNDi-1 std.	2.5	0.3	0.6	1.141830	0.000007	2.8	6.0	0.512096	0.000003	0.348404	0.000002	−6.1	4.5	0.241586	0.000002	−4.6	7.8	0.236463	0.000003	−5.8	10.9	0.72121	0.00032
JNDi-1 std.	3.1	0.2	0.1	1.141825	0.000006	−1.3	5.4	0.512095	0.000002	0.348407	0.000001	1.2	3.9	0.241587	0.000002	−0.7	6.8	0.236464	0.000002	−2.1	9.5	0.72163	0.00038
Average (n = 6)				1.141826	0.000006	0.0	5.5	0.512097	0.000005	0.348406	.000004	0.0	11.3	0.241587	0.000003	0.0	13.0	0.236464	0.000006	0.0	26.3	0.72187	0.00151
Allende run#1	1.5	3.8	0.9	1.141788	0.000009	−33.3	7.9	0.512674	0.000004	0.348405	0.000002	−3.4	6.8	0.241589	0.000003	4.7	10.8	0.236462	0.000003	−9.7	14.5	0.72121	0.00067
Allende run#3	2.7	1.4	3.4	1.141794	0.000007	−28.4	6.5	0.512672	0.000003	0.348406	0.000002	−0.1	4.9	0.241590	0.000002	8.9	7.9	0.236461	0.000003	−12.0	10.9	0.72261	0.00097
Average				1.141791	0.000008	−30.9	6.9	0.512673	0.000002	0.348406	0.000002	−1.7	4.7	0.241589	0.000001	6.8	6.1	0.236461	0.000001	−10.9	3.2	0.72191	0.00198
Jilin run#1	3.0	4.7	11.7	1.141801	0.000006	−22.4	5.3	0.512582	0.000002	0.348407	0.000001	2.8	4.2	0.241587	0.000002	−3.3	6.9	0.236460	0.000002	−17.2	9.6	0.72129	0.00091
Jilin run#2	2.6	0.8	11.3	1.141798	0.000006	−24.8	5.4	0.512580	0.000002	0.348408	0.000001	4.3	4.2	0.241589	0.000002	4.8	7.7	0.236460	0.000002	−16.1	9.9	0.72265	0.0005
Jilin run#3	2.5	0.6	14.0	1.141804	0.000007	−19.9	5.7	0.512580	0.000002	0.348407	0.000002	1.7	4.4	0.241590	0.000002	12.1	7.7	0.236464	0.000002	−0.6	10.4	0.7232	0.00014
Average				1.141801	0.000006	−22.4	5.0	0.512581	0.000003	0.348407	0.000001	2.9	2.6	0.241589	0.000004	4.5	15.5	0.236461	0.000004	−11.3	18.5	0.72238	0.00197

	Int. ^{142}Nd (V)	$^{142}Ce/^{142}Nd$ (ppm)	$^{144}Sm/^{144}Nd$ (ppm)	$^{142}Nd/^{144}Nd$	2s	$\mu^{142}Nd$ (ppm)	2s (ppm)	$^{143}Nd/^{144}Nd$	2s	$^{145}Nd/^{144}Nd$	2s	$\mu^{145}Nd$ (ppm)	2s (ppm)	$^{148}Nd/^{144}Nd$	2s	$\mu^{148}Nd$ (ppm)	2s (ppm)	$^{150}Nd/^{144}Nd$	2s	$\mu^{150}Nd$ (ppm)	2s (ppm)	$^{146}Nd/^{144}Nd$	2s
Sahara 97072 run1	4.6	1.0	4.8	1.141817	0.000005	−8.4	4.2	0.512550	0.000002	0.348406	0.000001	−0.7	3.3	0.241589	0.000001	7.1	5.6	0.236470	0.000002	27.2	8.0	0.72267	0.00065
Sahara 97072 run2	3.6	3.6	2.4	1.141810	0.000006	−14.0	4.9	0.512551	0.000002	0.348407	0.000001	0.7	3.7	0.241589	0.000002	6.3	6.3	0.236471	0.000002	27.5	8.7	0.72241	0.00048
Average				1.141814	0.000009	−11.2	8.0	0.512550	0.000001	0.348406	0.000001	0.0	2.1	0.241589	0.000002	6.7	1.1	0.236471	0.000000	27.4	0.4	0.72254	0.00037
Sahara 97096 run1	3.7	12.6	3.1	1.141805	0.000007	−18.8	5.8	0.512595	0.000003	0.348407	0.000002	1.4	4.4	0.241593	0.000002	23.1	7.7	0.236473	0.000002	36.4	10.5	0.72276	0.00076
Sahara 97096 run2	4.5	16.4	1.7	1.141801	0.000005	−22.6	4.3	0.512592	0.000002	0.348406	0.000001	0.4	3.2	0.241592	0.000001	18.5	5.8	0.236469	0.000002	21.8	7.5	0.72247	0.00022
Sahara 97096 run3	3.2	10.8	1.0	1.141803	0.000006	−20.6	5.0	0.512594	0.000002	0.348409	0.000001	7.8	3.9	0.241589	0.000002	6.2	6.9	0.236464	0.000002	−1.7	9.3	0.72302	0.00023
Sahara 97096 run4	3.2	9.1	1.2	1.141806	0.000006	−17.7	4.9	0.512595	0.000002	0.348406	0.000001	0.3	3.8	0.241591	0.000002	15.3	7.0	0.236468	0.000002	16.1	9.2	0.72383	0.00059
Average				1.141804	0.000005	−19.9	4.3	0.512594	0.000003	0.348407	0.000003	2.5	7.2	0.241591	0.000003	15.8	14.3	0.236468	0.000007	18.2	31.5	0.72302	0.00117
Sequence 3																							
JNDi-1 std.	7.1	0.7	0.5	1.141830	0.000004	−2.6	3.7	0.512102	0.000002	0.348401	0.000001	−0.4	2.7	0.241581	0.000001	−10.6	4.8	0.236452	0.000002	−22.7	6.6	0.72201	0.00032
JNDi-1 std.	6.4	0.7	0.4	1.141837	0.000004	3.1	3.7	0.512101	0.000002	0.348402	0.000001	0.4	2.9	0.241582	0.000001	−6.4	5.2	0.236458	0.000002	1.4	6.9	0.72191	0.00006
JNDi-1 std.	5.2	0.7	0.6	1.141837	0.000004	3.1	3.7	0.512101	0.000002	0.348402	0.000001	0.5	2.9	0.241582	0.000001	−6.6	5.0	0.236458	0.000002	1.5	6.8	0.72207	0.00031
JNDi-1 std.	8.4	0.2	0.3	1.141836	0.000004	2.8	3.3	0.512104	0.000001	0.348400	0.000001	−3.1	2.6	0.241581	0.000001	−9.6	4.3	0.236454	0.000001	−15.3	6.1	0.72259	0.00045
JNDi-1 std.	7.3	0.3	0.5	1.141836	0.000009	2.3	8.1	0.512104	0.000003	0.348400	0.000002	−3.6	6.4	0.241584	0.000003	1.0	10.8	0.236461	0.000003	12.6	14.0	0.72241	0.00023
JNDi-1 std.	6.1	0.2	0.5	1.141834	0.000008	1.0	6.9	0.512102	0.000003	0.348399	0.000002	−6.5	4.5	0.241581	0.000002	−9.0	9.3	0.236456	0.000003	−6.1	13.6	0.72266	0.00021
JNDi-1 std.	5.6	0.4	0.3	1.141828	0.000004	−4.4	3.9	0.512098	0.000002	0.348401	0.000001	−1.9	3.0	0.241586	0.000001	11.2	5.5	0.236461	0.000002	14.0	7.4	0.72329	0.00039
JNDi-1 std.	4.2	0.6	0.6	1.141833	0.000005	−0.4	4.4	0.512099	0.000002	0.348402	0.000001	2.1	3.5	0.241583	0.000001	−0.9	5.9	0.236455	0.000002	−13.0	8.1	0.72123	0.00055
JNDi-1 std.	8.0	0.0	0.6	1.141832	0.000004	−1.2	3.4	0.512098	0.000001	0.348402	0.000001	0.9	2.5	0.241584	0.000001	0.1	4.3	0.236459	0.000001	5.1	6.1	0.72339	0.00085
JNDi-1 std.	4.6	0.2	1.0	1.141836	0.000005	2.5	4.8	0.512103	0.000002	0.348403	0.000002	5.4	5.0	0.241585	0.000002	5.3	7.0	0.236460	0.000003	11.0	11.0	0.72231	0.00021
JNDi-1 std.	6.5	0.7	0.9	1.141835	0.000004	1.5	3.5	0.512099	0.000002	0.348403	0.000001	4.9	3.5	0.241586	0.000001	10.4	6.1	0.236459	0.000002	5.6	7.8	0.72191	0.00006
JNDi-1 std.	3.6	0.7	0.2	1.141828	0.000005	−4.9	4.1	0.512095	0.000002	0.348402	0.000001	2.5	3.7	0.241587	0.000002	15.1	6.5	0.236462	0.000002	16.4	8.3	0.72195	0.00011
JNDi-1 std.	4.2	0.5	0.7	1.141830	0.000004	−2.8	3.8	0.512096	0.000002	0.348401	0.000001	−1.2	3.6	0.241584	0.000002	0.1	6.2	0.236455	0.000002	−10.5	8.5	0.72193	0.00007
Average ($n = 13$)				1.141833	0.000007	0.0	5.8	0.512100	0.000006	0.348401	0.000002	0.0	6.7	0.241584	0.000004	0.0	16.9	0.236458	0.000006	0.0	25.0	0.72228	0.00119
LaJolla std	6.8	0.8	0.7	1.141830	0.000007	−2.8	6.2	0.511843	0.000003	0.348401	0.000002	−1.2	4.3	0.241584	0.000002	1.7	7.9	0.236461	0.000003	5.2	11.2	0.7229	0.00024
LaJolla std	5.8	1.3	0.3	1.141838	0.000005	3.9	4.0	0.511845	0.000002	0.348399	0.000001	−6.5	2.9	0.241585	0.000001	4.5	5.2	0.236461	0.000002	3.2	7.3	0.72305	0.00036
LaJolla std	7.0	1.1	0.3	1.141837	0.000005	3.0	4.4	0.511846	0.000002	0.348401	0.000001	−0.5	3.5	0.241583	0.000002	−0.8	6.5	0.236461	0.000002	2.4	8.1	0.72275	0.00039
LaJolla std	7.3	1.4	0.3	1.141831	0.000004	−2.1	3.5	0.511846	0.000002	0.348401	0.000001	−0.2	2.8	0.241583	0.000001	−2.1	4.5	0.236458	0.000001	−10.8	6.2	0.72245	0.00022
Average (n=4)				1.141834	0.000008	0.5	6.9	0.511845	0.000003	0.348401	0.000002	−2.1	5.9	0.241584	0.000001	0.8	5.8	0.236460	0.000004	0.0	14.6	0.72279	0.00051
AMES std	9.1	0.5	0.0	1.141832	0.000004	−0.6	3.2	0.511959	0.000001	0.348403	0.000001	3.4	2.3	0.241584	0.000001	−0.3	4.3	0.236457	0.000001	6.8	5.5	0.72265	0.00069
AMES std	8.5	1.2	0.0	1.141835	0.000004	1.4	3.1	0.511961	0.000001	0.348402	0.000001	1.2	2.5	0.241583	0.000001	−2.8	4.3	0.236457	0.000001	6.4	5.6	0.72207	0.00039
AMES std	7.8	1.0	−0.2	1.141830	0.000004	−2.6	3.3	0.511959	0.000002	0.348402	0.000001	1.8	2.5	0.241582	0.000001	−6.5	4.6	0.236455	0.000001	−5.1	6.1	0.72022	0.00055
AMES std	6.3	1.7	−0.1	1.141826	0.000004	−6.1	3.7	0.511958	0.000002	0.348401	0.000001	−0.7	3.0	0.241581	0.000001	−9.3	5.1	0.236454	0.000002	−6.3	6.6	0.71986	0.00047
AMES std	5.7	0.9	−0.2	1.141837	0.000005	3.6	4.0	0.511959	0.000002	0.348401	0.000001	−0.7	2.9	0.241582	0.000001	−4.8	5.3	0.236458	0.000002	7.7	7.0	0.72152	0.00045
AMES std	4.2	0.9	0.0	1.141831	0.000004	−1.6	3.2	0.511959	0.000001	0.348402	0.000001	2.1	2.5	0.241582	0.000001	−6.2	4.4	0.236457	0.000001	3.4	5.9	0.72187	0.00037
AMES std	5.2	2.0	−0.1	1.141832	0.000005	−1.1	4.0	0.511960	0.000002	0.348400	0.000001	−3.9	2.8	0.241580	0.000001	−15.2	5.0	0.236453	0.000002	−12.9	7.5	0.71964	0.00011
Average ($n = 8$)				1.141832	0.000007	−1.0	6.1	0.511959	0.000002	0.348402	0.000002	0.4	4.9	0.241582	0.000002	−6.4	9.6	0.236456	0.000004	0.0	16.1	0.72112	0.00239

Table S3. Measured Sm isotope composition of standards and samples

Sm isotope ratios normalized to $^{147}Sm/^{152}Sm = 0.56081$

	Int. 152Sm	$^{146}Nd/^{152}Sm$	$^{156}Gd/^{152}Sm$	$^{144}Sm/^{152}Sm$	2 s	$^{148}Sm/^{152}Sm$	2 s	$^{149}Sm/^{152}Sm$	2 s	$^{150}Sm/^{152}Sm$	2 s	$^{154}Sm/^{152}Sm$	2 s
Sequence 1	(V)	ppm	ppm										
Standard Sm	2.96	0.48	7.35	0.114975	0.000001	0.420437	0.000002	0.516856	0.000002	0.275985	0.000001	0.850761	0.000004
Standard Sm	4.55	0.19	2.14	0.114976	0.000001	0.420438	0.000002	0.516859	0.000002	0.275985	0.000001	0.850760	0.000003
Standard Sm	4.71	0.12	1.85	0.114976	0.000001	0.420436	0.000002	0.516856	0.000002	0.275984	0.000001	0.850765	0.000003
Standard Sm	4.88	−0.90	1.45	0.114979	0.000001	0.420435	0.000002	0.516854	0.000002	0.275984	0.000001	0.850770	0.000003
Standard Sm	5.64	−0.14	0.62	0.114980	0.000001	0.420434	0.000001	0.516853	0.000001	0.275983	0.000001	0.850777	0.000003
Average ($n = 5$)				0.114977	0.000004	0.420436	0.000003	0.516856	0.000005	0.275984	0.000002	0.850767	0.000014
2 s ppm				35.9		7.3		9.2		7.6		16.9	
Eagle	0.34	28.60	−4.90	0.114982	0.000014	0.420417	0.000014	0.516836	0.000015	0.275994	0.000011	0.850792	0.000021
Indarch	1.84	33.30	2.79	0.114979	0.000003	0.420431	0.000006	0.516833	0.000006	0.276008	0.000003	0.850781	0.000010
Kairpur	0.63	38.30	−3.12	0.114982	0.000011	0.420440	0.000011	0.516805	0.000012	0.276009	0.000010	0.850790	0.000018
Kota-Kota	0.77	35.40	1.62	0.114977	0.000005	0.420422	0.000008	0.516883	0.000008	0.275979	0.000006	0.850751	0.000015
MAC 02839	0.31	11.90	58.60	0.114991	0.000013	0.420434	0.000016	0.516820	0.000017	0.276012	0.000012	0.850833	0.000024
St. Mark's	0.36	30.90	11.10	0.114997	0.000014	0.420454	0.000015	0.516856	0.000018	0.275977	0.000012	0.850766	0.000030
Sahara 97096	0.36	20.80	9.88	0.114980	0.000014	0.420422	0.000012	0.516797	0.000012	0.276041	0.000011	0.850825	0.000020
Sequence 2													
Standard Sm	1.92	1.82	11.20	0.114978	0.000001	0.420428	0.000003	0.516856	0.000003	0.275982	0.000002	0.850769	0.000005
Standard Sm	2.65	0.60	1.42	0.114979	0.000001	0.420427	0.000002	0.516855	0.000002	0.275984	0.000001	0.850769	0.000003
Standard Sm	3.20	0.56	8.25	0.114978	0.000001	0.420428	0.000001	0.516855	0.000002	0.275982	0.000001	0.850756	0.000003
Standard Sm	2.70	0.74	6.36	0.114978	0.000001	0.420428	0.000001	0.516855	0.000001	0.275983	0.000002	0.850765	0.000016
Average ($n = 5$)				0.114978	0.000001	0.420428	0.000001	0.516855	0.000001	0.275983	0.000002	0.850765	0.000013
2 s ppm				5.5		1.6		1.9		7.1		15.0	
Hvittis	1.38	28.90	8.68	0.114982	0.000002	0.420425	0.000003	0.516821	0.000003	0.276047	0.000002	0.850782	0.000005
MAC 88180	1.70	5.91	1.88	0.114984	0.000001	0.420433	0.000002	0.516883	0.000003	0.275985	0.000002	0.850757	0.000004
Sahara 97158	0.59	26.40	51.70	0.114975	0.000005	0.420444	0.000004	0.516838	0.000005	0.276018	0.000004	0.850805	0.000008

Sm isotope ratios normalized to $^{147}Sm/^{154}Sm = 0.65918$

	$^{144}Sm/^{154}Sm$	2 s	$^{148}Sm/^{154}Sm$	2 s	$^{149}Sm/^{154}Sm$	2 s	$^{150}Sm/^{154}Sm$	2 s	$^{152}Sm/^{154}Sm$	2s
Sequence 1										
Standard Sm	0.135142	0.000001	0.494185	0.000002	0.607518	0.000003	0.324396	0.000002	1.175415	0.000004
Standard Sm	0.135143	0.000001	0.494186	0.000002	0.607522	0.000002	0.324396	0.000001	1.175416	0.000003
Standard Sm	0.135143	0.000001	0.494184	0.000002	0.607517	0.000002	0.324394	0.000001	1.175411	0.000003
Standard Sm	0.135147	0.000001	0.494182	0.000002	0.607514	0.000002	0.324394	0.000001	1.175406	0.000003
Standard Sm	0.135149	0.000001	0.494180	0.000002	0.607511	0.000002	0.324391	0.000001	1.175399	0.000003
Average ($n = 5$)	0.135145	0.000006	0.494183	0.000005	0.607516	0.000008	0.324394	0.000005	1.175410	0.000014
2s ppm	42.4		9.4		13.0		14.2		12.2	
Eagle	0.135155	0.000016	0.494159	0.000017	0.607483	0.000019	0.324400	0.000013	1.175384	0.000021
Indarch	0.135147	0.000004	0.494176	0.000007	0.607486	0.000007	0.324419	0.000004	1.175395	0.000010
Kairpur	0.135153	0.000012	0.494186	0.000013	0.607450	0.000016	0.324424	0.000011	1.175387	0.000018
Kota-Kota	0.135144	0.000006	0.494169	0.000009	0.607551	0.000010	0.324391	0.000007	1.175425	0.000014
MAC 02839	0.135164	0.000015	0.494176	0.000019	0.607450	0.000021	0.324414	0.000014	1.175343	0.000024
St. Mark's	0.135171	0.000016	0.494202	0.000017	0.607521	0.000019	0.324393	0.000014	1.175410	0.000030
Sahara 97096	0.135150	0.000016	0.494165	0.000015	0.607438	0.000016	0.324460	0.000014	1.175352	0.000020
Sequence 2										
Standard Sm	0.135145	0.000002	0.494174	0.000003	0.607517	0.000003	0.324391	0.000002	1.175407	0.000005
Standard Sm	0.135146	0.000001	0.494174	0.000002	0.607516	0.000002	0.324394	0.000001	1.175408	0.000003
Standard Sm	0.135146	0.000001	0.494175	0.000002	0.607518	0.000002	0.324394	0.000001	1.175421	0.000003
Standard Sm	0.135146	0.000001	0.494175	0.000002	0.607518	0.000002	0.324394	0.000001	1.175421	0.000003
Average ($n = 5$)	0.135146	0.000001	0.494175	0.000002	0.607517	0.000002	0.324393	0.000003	1.175414	0.000015

Sm isotope ratios normalized to $^{147}Sm/^{154}Sm = 0.65918$

	$^{144}Sm/^{154}Sm$	2 s	$^{148}Sm/^{154}Sm$	2 s	$^{149}Sm/^{154}Sm$	2 s	$^{150}Sm/^{154}Sm$	2 s	$^{152}Sm/^{154}Sm$	2s
2 s ppm	6.0		3.9		3.0		9.8		13.1	
Hvittis	0.135151	0.000002	0.494170	0.000004	0.607473	0.000004	0.324463	0.000003	1.175392	0.000006
MAC 88180	0.135152	0.000001	0.494181	0.000003	0.607550	0.000003	0.324397	0.000002	1.175419	0.000004
Sahara 97158	0.135147	0.000005	0.494187	0.000006	0.607491	0.000007	0.324427	0.000005	1.175363	0.000010

Table S4. The $^{142}Nd/^{144}Nd$ ratios are expressed in ppm deviation from the value obtained for the JNdi-1 terrestrial standard

Sample name	$^{142}Nd/^{144}Nd$ measured *	2σm †	$^{147}Sm/^{144}Nd$ measured ‡	$^{142}Nd/^{144}Nd$ corr. §	$^{147}Sm/^{144}Nd$ cal. ¶	$^{142}Nd/^{144}Nd$ corr. ‖	Reference
Abee	−43.6	17.1	0.1903	−35.4	0.1946	−41.5	(1)
ALHA77295	−2.3	7.4	0.1970	−3.6	0.1952	−1.2	this study
Eagle	−10.9	6.0	0.2001	−16.8	0.1982	−14.1	this study
Hvittis	−1.8	5.5	0.2007	−8.6	0.2000	−7.5	this study
Indarch	−14.6	5.0	0.1934	−10.9	0.1958	−14.3	(2)
Indarch	−17.7	7.4	0.2009	−24.8	0.1958	−17.4	this study
Khairpur	−13.2	5.1	0.1965	−13.9	0.1961	−13.4	this study
Kota-Kota	2.4	4.4	0.1675	43.3	0.1903	10.6	this study
MAC 02837	−4.4	0.3	0.1987	−8.2	0.1967	−5.4	this study
MAC 02839	−4.2	2.1	0.1976	−6.5	0.1964	−4.7	this study
MAC 88180	3.1	4.8	0.1974	1.1	0.1993	−1.7	this study
Sahara 97072	−16.1	4.3	0.1875	−3.9	0.1923	−10.8	this study
Sahara 97096	−19.9	4.3	0.1961	−20.0	0.1948	−18.2	this study
Sahara 97158	−13.9	9.9	0.1899	−5.1	0.1937	−10.7	this study
St. Mark's	−17.0	5.9	0.1953	−16.0	0.1951	−15.7	this study

*The $^{142}Nd/^{144}Nd$ ratios corrected for isobaric interferences and mass fractionation.

†Internal errors.

‡Measured $^{147}Sm/^{144}Nd$ ratios.

§The $^{142}Nd/^{144}Nd$ ratios corrected for a common evolution considering a constant $^{147}Sm/^{144}Nd$ ratio [0.196, (3)] from 4.568 Ga and an initial solar system $^{146}Sm/^{144}Sm$ ratio equal to 0.0085 (4). We have used the measured $^{147}Sm/^{144}Nd$ ratios.

¶The $^{147}Sm/^{144}Nd$ ratios calculated from measured $^{143}Nd/^{144}Nd$ ratios assuming that all meteorites evolve from the same chondritic reservoir since 4.568 Ga.

‖Corrected $^{142}Nd/^{144}Nd$ ratios following the method explained above but using calculated $^{147}Sm/^{144}Nd$ ratios instead of measured ratios. Note that the measured and calculated $^{142}Nd/^{144}Nd$ deviations are similar considering the analytical errors except for Kota-Kota, which is characterized by unusual low $^{147}Sm/^{144}Nd$ and $^{143}Nd/^{144}Nd$ ratios.

1 Boyet M, Carlson RW (2005) ^{142}Nd evidence for early (>4.53 Ga) global differentiation of the silicate earth. *Science* 309:576–581.
2 Carlson RW, Boyet M, Horan MF (2007) Chondrite barium, neodymium, and samarium isotopic heterogeneity and early earth differentiation. *Science* 316:1175–1178.
3 Bouvier A, Vervoort JD, Patchett PJ (2008) The Lu–Hf and Sm–Nd isotopic composition of CHUR: Constraints from unequilibrated chondrites and implications for the bulk composition of terrestrial planets. *Earth Planet Sci Lett* 273:48–57.
4 Boyet M, Carlson RW, Horan M (2010) Old Sm–Nd ages for cumulate eucrites and redetermination of the solars system initial $^{146}Sm/^{144}Sm$ ratio. *Earth Planet Sci Lett* 291:172–181.